

Effects of Salts and Ethanol on the Population and Morphology of Triblock Copolymer Micelles in Solution

A. G. Denkova,[†] E. Mendes,[†] and M.-O. Coppens^{*,†,‡}

DelftChemTech, Delft University of Technology, Julianalaan 136, 2628 BL Delft, The Netherlands, and Isermann Department of Chemical and Biological Engineering, Rensselaer Polytechnic Institute, 110 8th Street, Troy, New York 12180

Received: July 1, 2007; In Final Form: October 10, 2007

The morphological changes of micelles composed of triblock copolymer of ethylene oxide and propylene oxide (EO₂₀PO₇₀EO₂₀) in the presence of different inorganic salts and ethanol have been investigated using dynamic light scattering (DLS), rheometry, and cryogenic transmission electron microscopy (cryo-EM). The following salts were studied: KF, KCl, KI, LiCl, and CsCl. In the presence of KF, KCl, and CsCl, spherical and wormlike micelles coexist. LiCl and KI have little influence on the morphology of the micelles, whereas KF has the most pronounced effect. In agreement with the well-known Hoffmeister anion salt series, F[−] has the strongest effect of the three anions studied (F[−], Cl[−], I[−]). In contrast, the effectiveness of the cation type does not follow the original Hoffmeister cation series. The addition of ethanol to the KCl micellar solutions leads to the formation of more or longer wormlike micelles, which start to interact at certain copolymer concentrations depending on the volume fraction of ethanol added. Both the dilute and the semidilute regimes of the wormlike micelles were studied. The length of the micelles reaches a maximum value at around 8–10 vol % ethanol, after which it decreases again. At higher ethanol concentrations (18 vol %), spherical micelles are formed. Conclusions from this study enhance our understanding of the role played by ethanol and salts in the formation of micelle-templated mesoporous materials, such as SBA-15.

Introduction

Because of their ability to act as surfactants, amphiphilic triblock copolymers are often used as templating agents in the synthesis of large-pore mesoporous silicas and other inorganic oxides. Pores of an almost identical size appear after removal of the surfactants by extraction or calcination. Depending on the type of surfactant and the reaction conditions (temperature, pH, additives, stirring rate, and so on), ordered or disordered mesoporous silicas with different pore sizes and pore network topologies can be prepared.^{1,2} The formation mechanism of these materials is insufficiently clear, despite the numerous syntheses carried out by various research groups. Discoveries of new materials are often serendipitous, and researchers also disagree on the influence of experimental conditions on the end product. One example is the addition of salts to the reactants, which has been claimed to enhance the formation of rodlike particles.³ Sayari et al., however, argued that the formation of these particles is mostly due to the absence of stirring during material synthesis.⁴ This debate in the literature has triggered our interest in studying the influence of additives on the morphology of the amphiphilic triblock copolymer assemblies, rather than the final properties of the silica materials. Understanding the fundamental interactions between the templating agent and the various reactants should be useful in elucidating the formation mechanism of templated oxides and would lead to better-controlled syntheses and, ultimately, to the rational design of new mesoporous materials.

Triblock copolymer solutions have been studied extensively in the past, even long before the discovery of large-pore mesoporous silicas.⁵ The most frequently used block copolymers consist of ethylene oxide (EO) as end blocks and propylene oxide (PO) as the middle block and can be written with the general formula (EO)_m(PO)_n(EO)_m, where *m* and *n* are the numbers of EO and PO monomer units per block, respectively. At low temperatures, aqueous solutions of these polymers consist of unimers, which self-assemble to form micelles as temperature or concentration is increased.⁶ The core of the micelles is composed of PPO chains, and the PEO is situated in the corona.

Inorganic salts such as KF and KCl are known to decrease the temperature of micellization of these non-ionic surfactants, whereas salts such as KSCN and KI have exactly the opposite effect.^{7,8} The different salts have been classified in the so-called Hoffmeister or lyotropic series according to their “salting out” power. Specifically, for PEO, the cation lyotropic series seems to deviate from the original Hoffmeister series.⁹ For anions, the series is SO₄^{2−} > HPO₄^{2−} > F[−] > Cl[−] > Br[−] > I[−] > SCN[−]. The cation effect is usually less pronounced; this series is Cs⁺ ≈ Rb⁺ ≈ K⁺ > Na⁺ > Li⁺ > H⁺. In this case, the SO₄^{2−} and Cs⁺ ions have the strongest salting-out effect. The influence of these salts is attributed to the change in water structure resulting from the interactions between salts and water.¹⁰ F[−], for example, is called a “structure maker” because it increases the self-hydration of water through H-bonding. If the interactions between water molecules are stronger, less water will be available to hydrate the block copolymers, and the solubility of the latter will be reduced. However, there is no clear understanding yet of the roles of the different cations and anions. The effects of salts and elevated temperatures have been studied for the triblock copolymer P85, i.e., (EO)₂₇(PO)₃₉(EO)₂₇.⁷ It has

* To whom correspondence should be addressed. Present address: Isermann Department of Chemical and Biological Engineering, Rensselaer Polytechnic Institute, 110 8th Street, Troy, NY 12180. E-mail: Coppens@rpi.edu.

[†] Delft University of Technology.

[‡] Rensselaer Polytechnic Institute.

been shown that the initially spherical micelles undergo a sphere-to-rod transition when KF is added and the temperature is increased. Recently, Aswal et al. studied the same triblock copolymer in the presence of high salt concentrations but at much lower temperatures, confirming the formation of rodlike micelles.¹¹ Ganguly et al. demonstrated that, in the presence of a significant amount of NaCl and ethanol, the triblock copolymer P123, i.e., (EO)₂₀(PO)₇₀(EO)₂₀, can form micellar rods at room temperature.¹² The influence of ethanol is particularly interesting because it is usually formed, and in some cases added, during the synthesis of mesoporous silicas.^{3,4} One of the most common silica sources, for example, is tetraethyl orthosilicate (TEOS), which releases ethanol during hydrolysis and condensation.

Although our particular interest lies in the use of Pluronics as templating agents, these block copolymers are widely applied in detergency, emulsification, pharmaceuticals, separations, and the formulation of cosmetics.^{13–15} Additive-induced changes in triblock copolymer phase behavior can have a dramatic effect on the desired product properties.

For all of these reasons, in this study, we investigate in more detail the effect of ethanol on the morphological changes of P123 micelles in the presence of KCl. Additionally, we examine the separate influences of inorganic salts containing different anions and cations. Dynamic light scattering and rheometry are the primary techniques employed to study the morphological changes and the dynamical behavior of the P123 solutions, in both the dilute and semidilute regimes. We chose this triblock copolymer intentionally because it is one of the most commonly used in the synthesis of mesoporous silica materials such as SBA-15, as well as in a range of other applications.

Theory

The behavior of wormlike micelles closely resembles that of linear polymer solutions, and several analogies between the two can be made from a theoretical point of view. There are, however, at least two significant differences: First, because of their self-assembling character, polymer micelles can exhibit a large distribution of micellar lengths, whereas the length of polymer chains can be fixed during synthesis or fractionation. Second, wormlike micelles can break and recombine at different time scales depending on the system and the experimental conditions, making the system dynamic.

Dilute Systems. Dynamic light scattering (DLS) is a technique that can be used to provide information on characteristic times, and, therefore, sizes, associated with micellar assemblies. DLS allows one to measure the autocorrelation function, $g^{(2)}(\tau)$, of the scattered light intensity fluctuations detected in a small volume of solution in the microsecond time range

$$g^{(2)}(\tau) = \langle I(t) \cdot I(t + \tau) \rangle / \langle I(t) \rangle^2 \quad (1)$$

where I is the intensity and τ is the delay time. Polydisperse data are generally analyzed in two steps: First, the field autocorrelation function, $g^{(1)}(\tau)$, is estimated from the measured intensity autocorrelation function. The two autocorrelation functions are related by the Siegert equation

$$g^{(2)}(\tau) - 1 = \beta |g^{(1)}(\tau)|^2 \quad (2)$$

where β is an experimental coherence factor. $g^{(1)}(\tau)$ can be written as the integral over single-exponential decays with $G(\Gamma)$ as the decay distribution function and Γ as the decay or relaxation rate:

$$g^{(1)}(\tau) = \int_0^\infty G(\Gamma) \exp(-\Gamma\tau) d\Gamma \quad (3)$$

Formally, $g^{(1)}(\tau)$ is the Laplace transform of $G(\Gamma)$. Hence, the second step of the analysis involves the inverse Laplace transformation of eq 3 to find the distribution function $G(\Gamma)$. The widely applied Contin method uses this approach.¹⁶

The relaxation rate can also be obtained using the so-called cumulant expansion method.¹⁷ In the case of second-order cumulant analysis, the first derivative with respect to τ , i.e., Γ_1 , corresponds to the mean relaxation rate $\bar{\Gamma}$, and the second derivative, i.e., Γ_2 , corresponds to the variance of the relaxation rates, as follows

$$\ln[g^{(1)}(\tau)] = -\Gamma_1\tau + \frac{\Gamma_2\tau^2}{2!} + \dots \quad (4)$$

The average relaxation rate can be expressed according to the following equation, if the condition $qR_g < 5$ is fulfilled¹⁸

$$\frac{\bar{\Gamma}}{q^2} = D(1 + c'q^2R_g^2) \quad (5)$$

In eq 5, D is the average diffusion coefficient at a certain concentration, q is the norm of the scattering vector, R_g is the radius of gyration, and c' is a dimensionless value related to the structure of the micelles. The second term on the right-hand side can be omitted if $qR_g \ll 1$. In this case, the relaxation rate $\bar{\Gamma}$ divided by q^2 is approximately independent of the scattering vector.

When the reduced relaxation rate is plotted against the square of the norm of the scattering vector, q^2 , the apparent diffusion coefficient can be obtained from the intercept.

The dependence of the diffusion coefficient on the micellar volume fraction, ϕ , can provide useful information about the intermicellar interactions

$$D = D_0(1 + k_d\phi) \quad (6)$$

In this equation, D_0 is the diffusion coefficient extrapolated to infinite dilution, and k_d is the so-called diffusion virial coefficient. The diffusion virial coefficient can provide information on the nature and strength of the micellar interactions.

Subsequently, the apparent hydrodynamic radius can be calculated using the Stokes–Einstein equation

$$R_H = \frac{kT}{6\pi\eta D} \quad (7)$$

where k is the Boltzmann constant, T is the solvent temperature, and η is the solvent viscosity.

The length, L , of non-interacting, freely rotating rodlike micelles can be obtained from the hydrodynamic radius measured by DLS using Perrin's formula for a prolate ellipsoid with semimajor axis a and semiminor axis b , where $a > b$

$$R_H = \frac{a\sqrt{1 - (b/a)^2}}{\ln\left[\frac{1 + \sqrt{1 - (b/a)^2}}{b/a}\right]} \quad (8)$$

Here, the semiminor axis is given by $b = (d/2)\sqrt{3/2}$, where d is the diameter of the spherical micelle before the uniaxial micellar growth occurs. The semimajor axis, a , is equal to $L/2$.¹⁹

Semidilute Systems. At higher surfactant concentrations, above the so-called overlap concentration c^* , the micelles start

to interact and form a dynamic network characterized by a correlation length ξ (mesh size). In the semidilute regime, the diffusion coefficient obtained by dynamic light scattering is actually the collective diffusion coefficient. The Stokes–Einstein equation can be applied here as well, except that, in this case, the hydrodynamic radius, R_H , is replaced by the correlation length ξ .

It has been shown that the properties of semidilute wormlike micellar solutions can be described using scaling theories normally applied to entangled polymer systems, provided that measurements are made over a time scale shorter than the breaking time for scission and recombination.^{20,21} de Gennes showed that the dynamical properties of such solutions can be expressed in terms of the correlation length.²² Theoretically, the correlation length and, consequently, the collective diffusion coefficient (D_c) follow scaling laws according to

$$\xi \sim c^{-0.77} \quad \text{or} \quad D_c \sim c^{0.77} \quad (9)$$

Experimental Section

Materials. The triblock copolymer Pluronic P123 was obtained from Sigma Aldrich. The structural composition of this polymer is HO(C₂H₄O)₂₀(C₃H₆O)₇₀(C₂H₄O)₂₀H. It has a number-average molecular weight of 5800 g/mol. P123 was used as received without further purification.

Analytical-grade ethanol and the inorganic salts were purchased from Merck and Sigma Aldrich, respectively. The water was doubly distilled.

Aqueous solutions containing P123 were prepared by weighing. The salts and ethanol were added to these solutions as needed. All solutions were stirred at ambient temperature for at least 24 h and left to equilibrate for 1 week prior to measurements. The original P123 solutions were filtered through a 0.22- μ m Millipore filter. The final solutions were not filtered, as filtering can affect micelle morphology. The solutions were centrifuged to remove remaining dust particles.

Dynamic Light Scattering. The DLS apparatus consisted of a JDS Uniphase 633 nm 35 mW laser, an ALV sp 125 s/w 93 goniometer, a fiber detector, and a Perkin-Elmer photon counter. An ALV-5000/epp correlator and software completed the setup. The scattering cells (3 mL cylindrical tubes with an internal diameter of 12 mm) were immersed in a temperature-regulated bath containing index-matching fluid (toluene). The intensity autocorrelation function, $g^{(2)}(\tau)$, was determined at different angles ranging from 45° to 150°. Measurements were performed at 20 °C with the exception of the 15 vol % EtOH samples, which were also measured at 35 °C. The refractive index of the solvents was determined with an ATR-SW refractometer from Schmidt + Haensch.

The autocorrelation function was usually analyzed by means of the cumulant method, if not specified otherwise. The Contin method was used initially to check bimodality of the measured samples. In the case of a bimodal relaxation rate distribution, the field correlation function was fitted using a double-exponential function

$$g^{(1)}(\tau) = A_s \exp(-\Gamma_s \tau) + A_f \exp(-\Gamma_f \tau) \quad (10)$$

where Γ_s and Γ_f are the relaxation rates of the slow and the fast modes, respectively, and A_s and A_f are the corresponding amplitudes. The quality of each fit was checked by the χ^2 test.

Rheology. The viscosities of the P123 solutions containing the different salts were measured using an Ubbelohde capillary

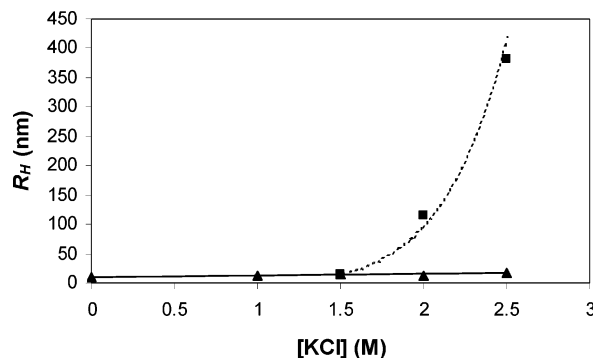


Figure 1. Variation of the apparent hydrodynamic radius obtained by DLS as a function of the KCl concentration for an aqueous solution containing 8×10^{-3} g/mL P123. Above about 1.5 M KCl, two different characteristic sizes were obtained.

viscometer. Oscillatory shear experiments were performed in the linear regime using a Rheometric Ares rheometer (Couette geometry).

Cryogenic Transmission Electron Microscopy (Cryo-EM).

Samples were prepared at room temperature by placing a droplet on a TEM grid. The extra liquid was then blotted with a filter paper, and the grid was inserted into liquid ethane at its melting point. The frozen samples were subsequently kept under liquid nitrogen. The TEM instrument used was a FEI Tecnai 20 FEG equipped with an imaging filter (Gatan 2001, with a $2K \times 2K$ CCD camera).

Results and Discussion

Anion Effect. Figure 1 shows the influence of the KCl concentration on the apparent hydrodynamic radius obtained by DLS. For the studied P123 concentration (8×10^{-3} g/mL), the correlation function exhibits a single relaxation time at low salt concentrations, as was observed previously in the case of salt-free aqueous P123 solutions ($\text{cmc} = 4 \times 10^{-3}$ wt % at 25 °C).⁶ The micelles in this case are expected to be spherical on the basis of their size (12.8 ± 0.4 nm at 1 M KCl), which is slightly larger than normal P123 micelles formed in pure water (9.0 ± 0.2 nm).²³ At higher salt concentrations (above 1.5 M KCl), two distinct relaxation times were detected corresponding to two different hydrodynamic radii (diffusion coefficients). These data were fitted using a double-exponential function according to eq 10. The objects having small characteristic sizes or large diffusion coefficient (D_{high}) can again be attributed to spherical micelles, as their size is very similar to that of the spherical micelles measured at lower KCl concentrations. The large surfactant assemblies (large R_H) have a much smaller diffusion coefficient (D_{low}). The existence of spherical micelles with such a large radius is highly improbable, considering the fact that the fully extended PEO and PPO chains for this polymer have a total length of approximately 28 nm.

Figure 2 displays the apparent diffusion coefficients of samples in pure water as well as in the presence of 2 M KI, 2 M KCl, and 0.6 M KF as a function of the surfactant concentration. The low KF concentration was chosen intentionally to avoid possible phase separation in the more concentrated P123 solutions. In the presence of 2 M KCl and 0.6 M KF, the relaxation rate distribution is bimodal (see Figure 1, Supporting Information). In this case, the light scattering data were fitted using the double-exponential function given by eq 10. Note that the relaxation rates of both the spherical micelles (fast mode) and the larger aggregates (slow mode) are linearly proportional to the squared norm of the scattering vector, q^2 , indicating that

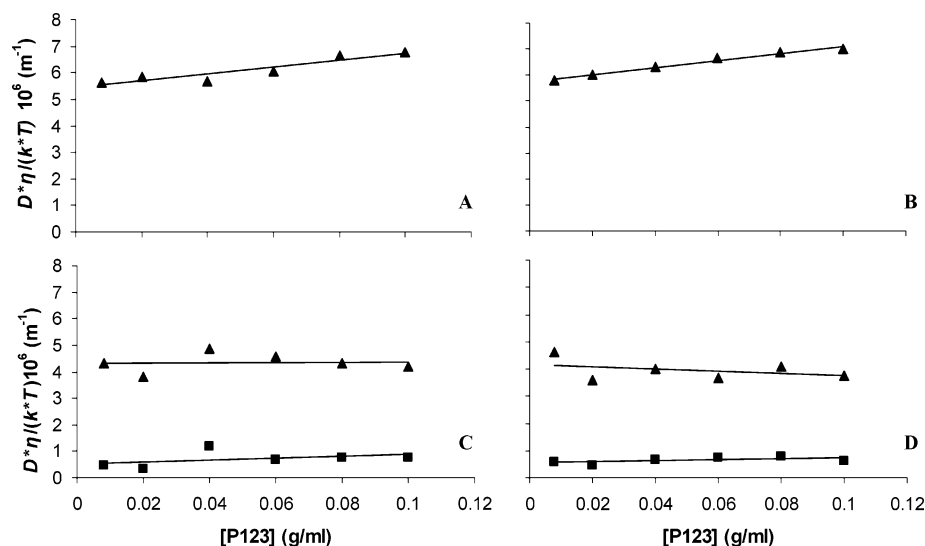


Figure 2. Variation of the reduced diffusion coefficient as a function of the P123 concentration in (A) pure H₂O, (B) 2 M KI, (C) 2 M KCl, and (D) 0.6 M KF. Spherical micelles are denoted by D_{high} (▲) and larger aggregates by D_{low} (■).

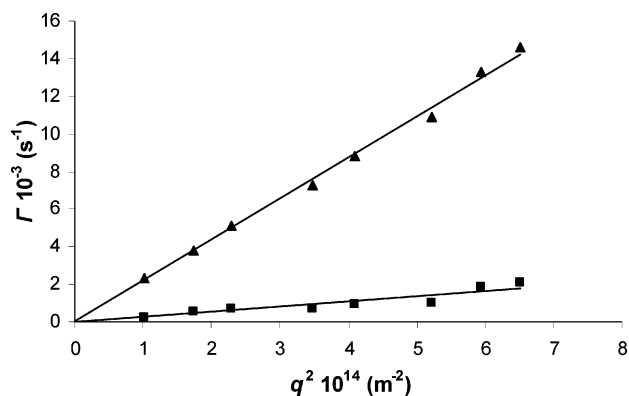


Figure 3. Fast (▲) and slow (■) relaxation rates as functions of q^2 for a sample containing 8×10^{-3} g/mL P123 in the presence of 2 M KCl. The lines are linear fits of the data.

the modes are diffusive, as shown in Figure 3. All bimodal distributions, up to the highest P123 concentrations, show this linear dependence. Semidilute wormlike solutions are also known to exhibit an additional slow relaxation mode, which is attributed to the structural changes of the transient network formed. However, such a viscoelastic relaxation mode in the semidilute regime is typically independent of the scattering vector.^{24,25} Clearly, the slow mode (low diffusion coefficient) measured here cannot be assigned to such a structural relaxation process. Rheometry results presented later in this article support the conclusion that the micelles are still in the dilute regime at all studied concentrations.

From Figure 2C and D, it can be seen that D_{high} is slightly lower than the value of the diffusion coefficient obtained in the salt-free situation. This indicates that the spherical micelles are larger in the presence of KCl and KF. The concentration dependence of the diffusion coefficient in Figure 2A and B can yield information on the type of micellar interactions. By applying eq 6, one can obtain the diffusion virial coefficient, which, in this case, is positive and equal to 2.36 for both the KI sample and the pure P123 sample. For this calculation, we assumed that the polymer volume fraction was equal to the volume fraction of the micelles. The positive virial coefficient indicates that the micelles have repulsive interactions. The theoretical diffusion virial coefficient for colloidal particles with hard-sphere interactions is 1.56.²⁶ In this study, the second virial

coefficient measured is 1.5 times larger than the theoretical value, which can be explained by the hydration of the PEO corona. As expected, the volume fraction of the dry polymer is less than that of the hydrated polymer fraction. Such a clear upturn was not detected in the presence of KCl and KF for either D_{low} or D_{high} . The slopes of these curves are notably less steep, indicating reduced repulsive interactions or even the presence of weak attractive forces.

Despite the large amount of KI added to the solutions, this salt seems to have no effect on the micelle morphology, as we detected one diffusion coefficient (Figure 2B) very close to that found in the pure P123 solutions.

The shape of the large aggregates cannot be deduced from the DLS measurements because of the polydispersity of the samples. However, cryo-EM images (Figure 4) taken of a sample containing 1×10^{-2} g/mL P123 and 1 M KF show that wormlike and spherical micelles coexist. The cryo-EM images exhibit some regions with many wormlike micelles and others consisting almost entirely of spherical micelles (Figure 4). The preparation conditions of the cryo-EM samples might be responsible for this effect. To achieve better-quality images, cryo-EM experiments were performed at slightly higher KF concentrations than those used in the DLS and rheology studies. At this low P123 concentration (1×10^{-2} g/mL), the difference between samples containing 0.6 and 1 M KF is not that significant. The only notable difference is that more wormlike micelles are formed as the KF concentration is increased. The cryo-EM images reveal that the diameter of the spherical micelles is larger than that of the cylindrical micelles. The diameter of the formed anisotropic micelles is known to decrease to some extent as a result of the sphere-to-rod transition.²⁷ The formation of wormlike micelles in the presence of both KCl and KF is additionally confirmed by the flow birefringence of the solutions. The simultaneous formation of wormlike and spherical micelles has also been observed for another triblock copolymer, P85, in the presence of high concentrations of salt.¹¹

In Figure 5, the amplitude of the slow relaxation mode obtained with the double-exponential fit according to eq 10 is displayed as a function of the scattering angle for three different samples. Two of the samples contain 2 M KCl and either 8×10^{-3} or 8×10^{-2} g/mL P123. The third sample contains 0.6 M KF and 8×10^{-3} g/mL P123. The amplitude of the slow mode can be used as a measure for the relative number of wormlike

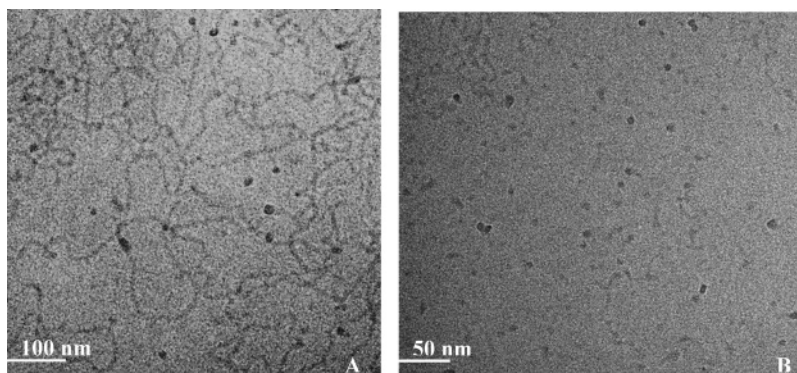


Figure 4. Cryo-EM image of a sample containing 1×10^{-2} g/mL P123 and 1 M KF: (A) wormlike micelles and (B) spherical micelles.

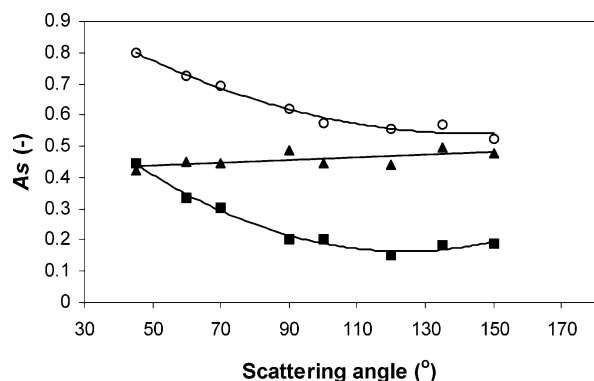


Figure 5. Variation of the slow-mode amplitude for a sample containing 2 M KCl and P123 at 8×10^{-3} g/mL (■) and 8×10^{-2} g/mL (▲) and a sample containing 0.6 M KF at 8×10^{-3} g/mL P123 (○).

micelles formed. The slow-mode amplitudes of the 8×10^{-3} g/mL P123 samples decrease with increasing scattering angle. Large objects scatter significantly at low angles, whereas at wider angles, their contribution to the scattered intensity is reduced. The presence of KF clearly leads to the formation of more cylindrical micelles than does the presence of KCl, as can be easily seen by comparing the slow-mode amplitudes (A_s) of the two samples at, for example, 90° . Assuming that the samples are in the dilute regime, we expect that their average length is comparable to the length of the micelles in the 2 M KCl case, given that the two diffusion coefficients are of the same order of magnitude, as can be seen in Figure 2C and D. In the presence of KCl and at higher P123 concentrations (8×10^{-2} g/mL), the amplitude of the slow mode, A_s , is larger, suggesting that more wormlike micelles are created as concentration increases. At this point, it should be emphasized that the number of wormlike micelles is probably less than proportional to the increase in A_s , as large objects contribute substantially more to the scattered intensity and, therefore, are always more pronounced in the light scattering unweighted distribution.

Figure 6A shows the relative viscosity (relative to the solvent) as a function of the P123 concentration for samples containing an aqueous solution of P123, pure and in the presence of KCl and KI. Figure 6B displays the relative viscosities of samples containing the triblock copolymer and KF. The same trend is observed here as in the DLS experiments. KI seems to have no significant effect, whereas the strongest viscosity increase is found in the presence of KF. The difference in viscosity between the salt-free solutions and the KCl-containing solution is surprisingly small. Wormlike micelles are expected to lead to a higher viscosity than spherical micelles, provided that the solutions are in the semidilute regime. The observed low

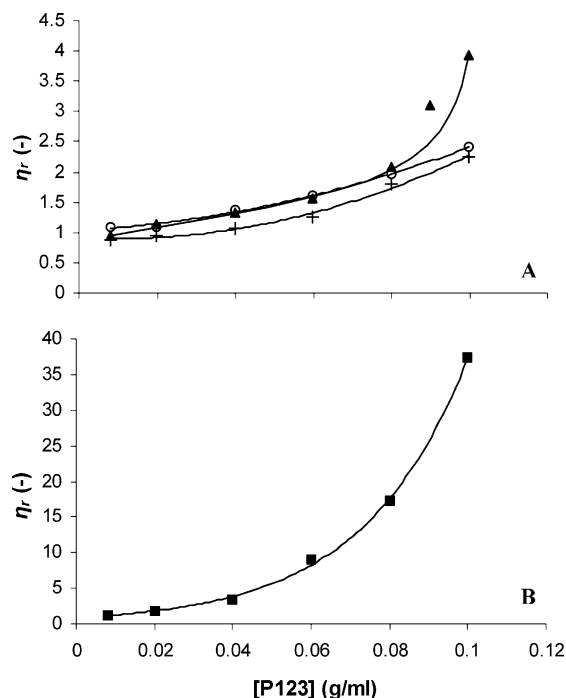


Figure 6. Relative viscosity as a function of the P123 concentration for samples containing (A) no salt (○), 2 M KCl (▲), and 2 M KI (+) and (B) 0.6 M KF (■).

viscosity is probably due to the small number of wormlike micelles at low P123 concentrations and the presence of spherical micelles. Solutions consisting of non-interacting wormlike micelles are not expected to be highly viscous. The small viscosity increase with increasing P123 concentration in the KCl case confirms that the micelles are still in the dilute regime. When KF is added to the micellar solution, the relative viscosity shows a significant jump with increasing surfactant concentration. This suggests that the wormlike micelles are in contact with each other. However, the micelles still seem to be in the dilute regime exhibiting liquidlike behavior (Figure 2 in the Supporting Information). Note that, at low P123 concentrations, all micellar solutions have similar viscosities, although in the KF case, many more wormlike micelles are likely to be present judging from the DLS results and the cryo-EM image recorded under similar conditions.

Scaling laws, characteristic for wormlike surfactant micelles in the semidilute regime, were not observed for any of the studied salt samples, which further verifies that the micelles are in the dilute regime.

The observed influence of the different anions closely follows the Hofmeister series. F^- ions have the most pronounced effect, whereas I^- ions seem to have no impact on the morphology of

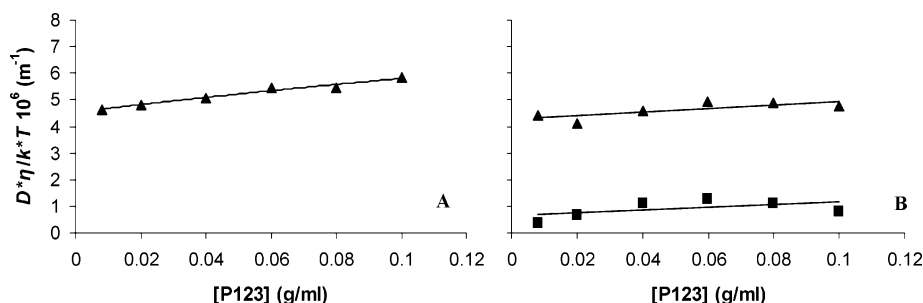


Figure 7. Variation of the reduced diffusion coefficient as a function of the P123 concentration in (A) 2 M LiCl and (B) 2 M CsCl. Spherical micelles are denoted by D_{high} (\blacktriangle) and wormlike micelles by D_{low} (\blacksquare).

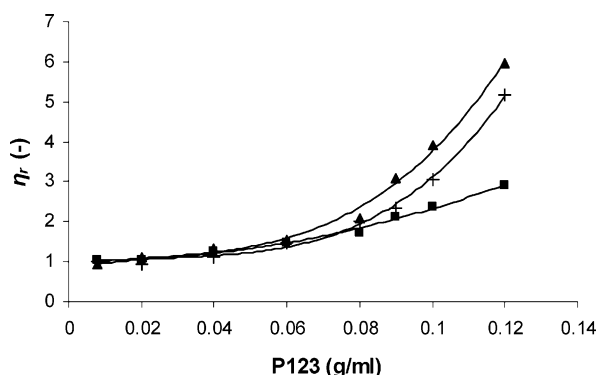


Figure 8. Relative viscosity as a function of P123 concentration for samples containing 2 M KCl (\blacktriangle), 2 M CsCl ($+$), and 2 M LiCl (\blacksquare).

the micelles. The influence of the I^- ions, could, however, be reduced by the presence of the structure maker K^+ ion.

Cation Effect. The influence of different cations on the micelle morphology was examined in a similar way. The results obtained by DLS for 2 M LiCl and 2 M CsCl are displayed in Figure 7A and B, respectively. In the presence of LiCl, no wormlike micelles are formed, although the spherical micelles are larger than the normal P123 micelles found in pure water (Figure 2A). The effect of CsCl (Figures 7 and 8) can be compared to that of KCl. Figure 8 shows the viscosity as a function of the P123 concentration for KCl, CsCl, and LiCl solutions.

Solutions containing KCl and CsCl have comparable viscosities, although the KCl samples are slightly more viscous. The samples containing LiCl have the lowest viscosity of the three salt solutions, which is expected because the micelles in this case are still spherical. The cation type seems to have less impact on the morphology of the micelles than the anion type. Likewise, for the micellization of triblock copolymers, the cation type used is not of major importance provided that all cations are monovalent.²⁸ Multivalent cations and anions are expected to have a larger salting-out power. Note that the presented effectiveness of the cation type ($\text{Cs}^+ \approx \text{K}^+ > \text{Li}^+$) strongly diverges from the original Hoffmeister series, which reads as follows: $\text{Ca}^{2+} > \text{Ba}^{2+} > \text{Li}^+ > \text{Na}^+ > \text{K}^+ > \text{Rb}^+ > \text{Cs}^+$.²⁹ According to the salting-out theory, the more hydrated the ion is, the more pronounced its effectiveness. In our study, we showed that Li^+ ions, which are highly hydrated, have little influence on the morphology of the micelles. Clearly, the salting-out potential of the different ions does not only depend on their hydration. Several research groups have already established that the cation influence on the salting out of PEO itself is not in accordance with the Hoffmeister series.^{9,30} The exact order of the cation series seems to depend on the counterion. Ataman showed that, in the case of Cl^- as the counterion, the series can be presented as $\text{Cs}^+ \approx \text{Rb}^+ \approx \text{K}^+ > \text{Na}^+ > \text{Li}^+ > \text{H}^+$.

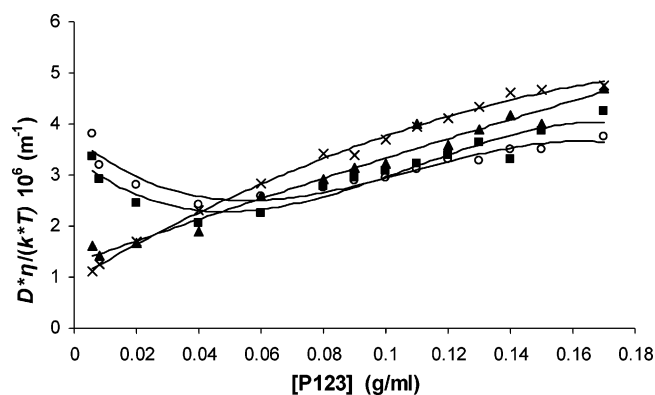


Figure 9. Variation of the reduced diffusion coefficient as a function of the P123 concentration in the presence of 2 M KCl and 3 (\circ), 5 (\blacksquare), 8 (\blacktriangle), and 10 (\times) vol % EtOH.

This is in direct agreement with our findings and is probably due to the fact that the corona of the micelles is composed of PEO. The dehydration of the corona is believed to be responsible for the formation of the wormlike micelles.

Ethanol Effect. The effect of solvent quality was also investigated by the addition of ethanol to the KCl micellar solutions. The relaxation rates of all ethanol-containing samples were analyzed using the cumulant method. In this case, the reduced diffusion coefficients of the micelles are depicted in Figure 9. At 3 and 5 vol % EtOH, the diffusion coefficient initially decreases with increasing P123 concentration. This decrease is associated with the growth of the micelles. Once the wormlike micelles reach a certain length, L^* , they start to overlap, forming a network characterized by a correlation length ξ , which is associated with the collective diffusion coefficient. This transition from the dilute to the semidilute regime is clearly observed at low ethanol concentrations, as depicted in Figure 9. In this case, as predicted, the diffusion coefficient first decreases with polymer concentration until the overlapping concentration c^* is reached, after which it increases again.

At higher ethanol concentrations (8 and 10 vol %), the micelles are close to the semidilute regime. The dependency of D_c on the surfactant concentration in the concentrated regime confirms the formation of a transient network of cylindrical micelles. Using the experimental data presented in Figure 9, the variation of D_c with polymer concentration could be fitted by a power law. For instance, for the sample containing 10 vol % EtOH, the fit reads $D_c \sim c^{0.6 \pm 0.03}$ (Figure 3, Supporting Information). This value is lower than that theoretically predicted for wormlike micelles in a good solvent (0.77).²² Deviations from the predicted exponent are not unusual and have also been observed for polymer systems consisting of short chains or containing bad solvents.³¹

Additionally, shape polydispersity of the micelles can affect the calculated exponent. However, we were not able to obtain

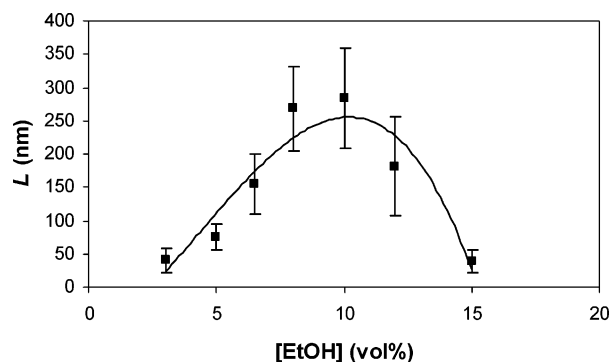


Figure 10. Variation of the micellar length L with the ethanol concentration for an 8×10^{-3} g/mL P123 solution containing 2 M KCl.

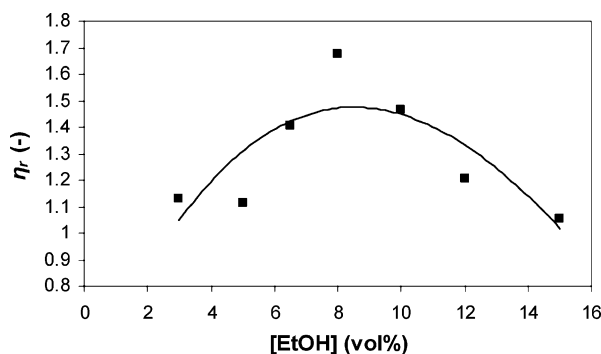


Figure 11. Variation of the relative zero-shear viscosity with the ethanol concentration for an 8×10^{-3} g/mL P123 solution containing 2 M KCl.

reliable fits of the light scattering data using a double-exponential function, which implies that the number of spherical micelles is insignificant or that any such micelles are caught in the transient micellar network and cannot be measured separately. The number of rods formed in the presence of ethanol is significantly larger than the number found in its absence, given that scaling laws were not found to be applicable when only KCl was added to the micellar solutions (see Figure 2C). However, the applicability of scaling laws to the salt solutions is not excluded at much higher P123 concentrations when the number of wormlike micelles is significant, provided that phase separation does not occur.

The effect of ethanol is surprising, considering that it is a good solvent for both the PO and EO chains and it is not expected to cause the formation of cylindrical micelles. It was established by Alexandridis et al. and verified by our own measurements that the apparent hydrodynamic radius of the triblock copolymer micelles in water decreases with increasing ethanol concentration.³² The reduction of the micelle size is attributed to the decrease in interfacial tension between the solvent and the hydrophobic PPO chains.

Using Perrin's formula (eq 8), we calculated the length of the micelles from their apparent hydrodynamic radius. These calculations were performed for a P123 concentration of 8×10^{-3} g/mL, assuming no interactions among the micelles. Therefore, in some cases (8, 10, and 12 vol % EtOH), the estimated length can be slightly smaller than the actual value.

Figure 10 shows that the micelles grow with increasing ethanol concentration until a maximum is reached, after which their length decreases again. The measured zero-shear viscosity supports this finding (Figure 11). The maximum length is reached around 8–10 vol % EtOH. The existence of a maximum length suggests that two processes are in competition. If ethanol

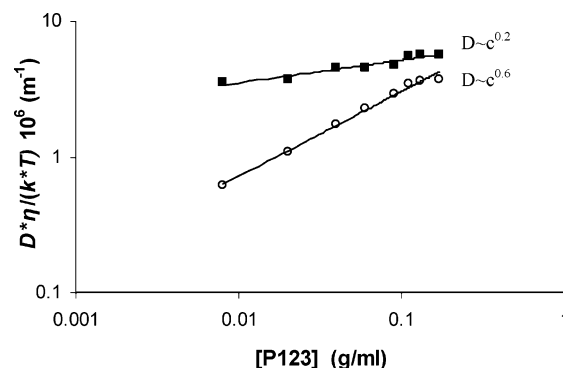


Figure 12. Variation of the reduced diffusion coefficient with the P123 concentration for a sample containing 2 M KCl and 15 vol % EtOH at 20 (■) and at 35 (○) °C.

were solely responsible for the formation of cylindrical micelles, one would expect that the addition of more ethanol would lead to longer micelles. Such behavior is typically observed when salt or temperature is the cause for elongation and branching effects are not interfering. In our case, the length of the micelles is evidently reduced at 15 vol % ethanol, and the measured diffusion coefficient varies little with concentration at room temperature as shown in Figure 12. Ethanol seems to improve the quality of the solvent, and as a result, smaller micelles are formed. A further increase of the ethanol concentration to 18 vol % causes the formation of spherical micelles with a radius of 8.7 ± 0.5 nm, completely negating the KCl effect. Ethanol is expected to preferably swell the micellar core, because it is a better solvent for the PPO chains than the PEO.³² The addition of salt, however, dehydrates the corona, forcing it to collapse. The combination of the two effects will drive the transition from sphere to rod, as long as ethanol does not start to swell the micellar corona. The addition of more ethanol will eventually lead to the distribution of ethanol in the core and the corona, canceling the dehydrating effect of the KCl. In fact, it can be speculated that any solvent that preferably solvates the core but is a good solvent for both PEO and PPO will have the same effect as ethanol.

To demonstrate the influence of ethanol on the solvent quality, we performed measurements at a higher temperature. The addition of certain salts (such as KF, KCl, etc.) and/or an increase of temperature induce dehydration of the EO chains of the corona, which, in turn, can lead to sphere-to-rod transition. This was demonstrated previously with the triblock copolymer P85.^{7,11} Figure 12 shows the reduced diffusion coefficient for P123 solutions containing 15 vol % EtOH at 20 and 35 °C. At 35 °C, the diffusion coefficient is visibly lower, and it scales with a power-law exponent of 0.6 ± 0.02 of the concentration. Data fitting with a power law should be carried out well above c^* , in order to determine the correct exponent. However, the plot in Figure 12 is used simply to demonstrate the difference between the two samples, and we chose to fit the data throughout the whole measured regime.

At 20 °C, the micelles are relatively short and do not resemble interacting polymer chains. These solutions do not exhibit any flow birefringence, which is normally found for wormlike micelles. An increase in temperature reduces the solvent quality and causes the creation and growth of anisotropic micelles. Rheological data support these observations. Figure 13 shows the storage modulus (G'), the loss modulus (G''), and the viscosity plotted against the angular frequency for a sample containing 0.1 g/mL P123, 2 M KCl, and 15 vol % EtOH at 20 and 35 °C. At 20 °C, the micelles have typical liquidlike

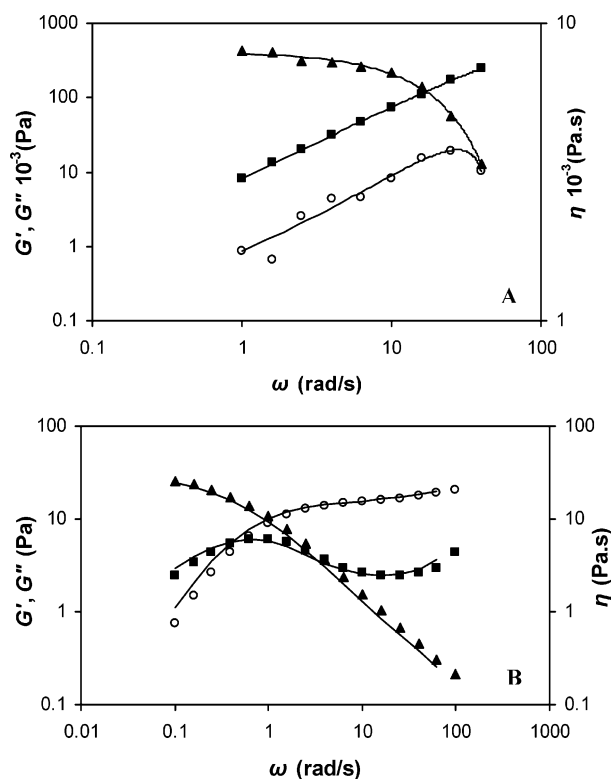


Figure 13. Storage modulus G' (○), loss modulus G'' (■), and viscosity η (▲) as functions of the angular frequency for a sample containing 0.1 g/mL P123, 2 M KCl, and 15 vol % EtOH at (A) 20 and (B) 35 °C.

behavior ($G'' > G'$) throughout the measured frequency range. At 35 °C, the sample has distinctive viscoelastic properties at low frequencies, whereas at higher frequencies, a gel-like behavior ($G' > G''$) is observed. The obtained curve is characteristic for a wormlike micellar solution.³³ Furthermore, the viscosity increases substantially between 20 and 35 °C.

Conclusions

Spherical micelles composed of the triblock copolymer P123 in water transform into wormlike micelles when certain salts such as KCl, KF, and CsCl are added. This transformation can be explained by the dehydration of the PEO chains in the micelle corona, which is considered to be the driving force for the sphere-to-rod transition in non-ionic surfactant systems.³⁴ In agreement with the Hoffmeister series, KF has the strongest effect of the three salts studied (KF, KCl, KI). The addition of KI does not lead to wormlike micelles. On the contrary, the spherical micelles are smaller than those found in the other salt solutions. The influence of the cation is less pronounced, although Li^+ clearly has the smallest effect of the three examined cations (Li^+ , Cs^+ , K^+). The effectiveness of the cation type does not follow the original Hoffmeister series, but it is in agreement with results obtained for PEO.

The syntheses of large mesoporous silica materials using P123 as a templating agent are normally carried out around 35–40 °C. Salts are sometimes added during the synthesis, and ethanol is normally formed as a result of the hydrolysis and condensation of tetraethyl orthosilicate (TEOS), a common silica precursor. At elevated temperatures, a small amount of the right salt will be sufficient to induce the formation of wormlike micelles, which can, in turn, result in a silica with a rodlike morphology. Silica precursors can have an effect similar to that of salt addition, removing water from the PEO chains and causing a

sphere-to-rod transition. In fact, water depletion from the PEO/water interface seems to take place during the synthesis of SBA-15, a silica synthesized using triblock copolymer micelles as templates for its ordered array of pores.³⁵ Although salts can facilitate the formation of wormlike micelles, we have shown that, in the absence of ethanol, spherical micelles are still present. This can result in a nonhomogeneous product. Ethanol, which can be seen as a byproduct of the synthesis, has an unexpectedly positive contribution in achieving a more homogeneous product. We have shown that its addition causes the formation of more or longer wormlike micelles. The optimal ethanol concentration corresponding to the maximum length of the wormlike micelles is around 8–10 vol %. Interestingly, the amount of ethanol formed during the synthesis of, e.g., SBA-15, when TEOS is used, is roughly estimated to be around 10 vol % or lower, provided that TEOS is completely hydrolyzed.³⁶ The presence of spherical micelles at the ethanol concentrations studied here is not excluded. However, their number is much lower than in the absence of ethanol.

The effect that small amounts of ethanol have on the morphology of the P123 micelles in the presence of a dehydrating source (salt and/or temperature) can be of significant importance for the application of P123 in other fields as well. The length of the wormlike micelles can be controlled by varying the solvent quality. This, in turn, affects the viscosity of the micellar solutions. Wormlike micelles are often used as thickeners in various consumer products where control of viscosity is essential. Additionally, there is a growing interest in the use of wormlike micelles for drug delivery. It is expected that drug release and distribution might be better controlled if cylindrical carriers were used.³⁷ Controlling the length of the wormlike micelles by changing solvent quality might be used to optimize drug release.

Acknowledgment. We gratefully acknowledge Dr. R. I. Koning and Dr. A. J. Koster (LUMC, Leiden, The Netherlands) for providing the cryo-EM image used in this article.

Supporting Information Available: Example of a bimodal correlation function and the corresponding CONTIN fit for a sample containing 6×10^{-2} g/mL P123 and 0.6 M KF. Variations of G' , G'' , and viscosity as functions of frequency for a sample containing 8×10^{-2} g/mL P123 and 0.6 M KF. Variation of the reduced diffusion coefficient with the P123 concentration for a sample containing 2 M KCl and 10 vol % EtOH, as obtained by DLS. This material is available free of charge via the Internet at <http://pubs.acs.org>.

References and Notes

- (1) Zhao, D.; Huo, Q.; Feng, J.; Chmelka, B. F.; Stucky, G. D. *J. Am. Chem. Soc.* **1998**, *120*, 6024.
- (2) Flodström, K.; Alfredsson, V.; Källrot, N. *J. Am. Chem. Soc.* **2003**, *125*, 4402.
- (3) Yu, C.; Fan, J.; Tian, B.; Zhao, D.; Stucky, G. D. *Adv. Mater.* **2002**, *14* (23), 1742.
- (4) Sayari, A.; Han, B. H.; Yang, Y. *J. Am. Chem. Soc.* **2004**, *126*, 14348.
- (5) Zhou, Z.; Chu, B. *J. Colloid Interface Sci.* **1988**, *126*, 171.
- (6) Wanka, G.; Hoffmann, H.; Ulbricht, W. *Macromolecules* **1994**, *27*, 4145.
- (7) Jorgensen, E. B.; Hvidt, S.; Brown, W.; Schillen, K. *Macromolecules* **1997**, *30* (8), 2355.
- (8) Alexandridis, P.; Holzwarth, J. F. *Langmuir* **1997**, *13*, 6074.
- (9) Ataman, M. *Colloid Polym. Sci.* **1987**, *265*, 19.
- (10) Luck, W. A. P. *Top. Curr. Chem.* **1974**, *64*, 113.
- (11) Aswal, V. K.; Wagh, A. H.; Kammel, M. *J. Phys. Condens. Matter* **2007**, *19*, 116101.
- (12) Ganguly, R.; Aswal, V. K.; Hassan, P. A.; Gopalakrishnan, I. K.; Yakhmi, J. V. *J. Phys. Chem. B* **2005**, *109*, 5653.

- (13) Guzman, M.; Garcia, F. F.; Molpeceres, J.; Aberturas, M. R. *Int. J. Pharm.* **1992**, *80*, 119.
- (14) Schmalk, I. R. *J. Am. Oil Chem. Soc.* **1977**, *54*, 110.
- (15) Bahadur, P.; Riess, G. *Tenside Surf. Det.* **1991**, *28*, 173.
- (16) Provencher, S. W. *Macromol. Chem.* **1979**, *180*, 201.
- (17) Mandel, M. In *Dynamic Light Scattering—The Method and Some Applications*; Brown, W., Ed.; Oxford Science Publishers: Oxford, U.K., 1993; p 326.
- (18) Burchard, W.; Schmidt, M.; Stockmayer, W. H. *Macromolecules* **1980**, *13*, 580.
- (19) Chu, B. *Laser Light Scattering*; Academic Press: London, 1974; p 212.
- (20) Candau, S. J.; Hirsch, E.; Zana, R. *J. Colloid Interface Sci.* **1985**, *105*, 521.
- (21) Buhler, E.; Munch, J. P.; Candau, S. J. *J. Phys. II* **1995**, *5*, 765.
- (22) de Gennes, P. G. *Scaling Concepts in Polymer Physics*; Cornell University Press, Ithaca, NY, 1979.
- (23) Nolan, S. L.; Phillips, R. J.; Cotts, P. M.; Dungan, S. R. *J. Colloid Interface Sci.* **1997**, *191*, 291.
- (24) Adam, M.; Delsanti, M. *Macromolecules* **1985**, *18*, 1760.
- (25) Brown, W. In *Dynamic Light Scattering—The Method and Some Applications*; Brown, W., Ed.; Oxford Science Publishers: Oxford, U.K., 1993; p 299.
- (26) Pusey, P. N.; Tough, R. J. A. In *Dynamic Light Scattering: Application of Photon Correlation Spectroscopy*; Pecora, R., Ed.; Plenum Press: New York, 1985.
- (27) Linse, P. *J. Phys. Chem.* **1993**, *97*, 13896.
- (28) Jain, N. J.; Aswal, V. K.; Goyal, P. S.; Bahadur, P. *Colloids Surf. A* **2000**, *173*, 85.
- (29) Shaw, D. J. *Introduction to Colloid and Surface Chemistry*; Butterworths: London, 1966; p 150.
- (30) Napper, N. H. *J. Colloid Interface Sci.*, **1970**, *33*, 384.
- (31) Schaefer, D. W.; Joanny, J. F.; Pincus, P. *Macromolecules* **1980**, *13*, 1280.
- (32) Alexandridis, P.; Yang, L. *Macromolecules* **2000**, *33*, 5574.
- (33) Rehage, H.; Hoffmann, H. *J. Phys. Chem.* **1988**, *92*, 4712.
- (34) Heeklotz, H.; Tsamaloukas, A.; Kita-Tokarczyk, K.; Strunz, P.; Gutberlet, T. *J. Am. Chem. Soc.* **2004**, *126*, 16544.
- (35) Ruthstein, S.; Schmidt, J.; Kesselman, E.; Talmon, Y.; Goldfarb, D. *J. Am. Chem. Soc.* **2006**, *128*, 3366.
- (36) Pitchumani, R.; Li, W.; Coppens, M.-O. *Catal. Today* **2005**, *105*, 618.
- (37) Kim, Y.; Dalhaimer, O.; Christian, D. A.; Discher, D. E. *Nanotechnology* **2005**, *16*, S484.